

Novel Aspects of Bounded Velocity Transport

F. Debbasch, D. Espaze and V. Foulonneau

Abstract—Stochastic models of bounded velocity transport are revisited. It is proven that these models exhibit short-time propagative (as opposed to diffusive) behavior for a large class of initial conditions. Numerical simulations also show that this propagative effect is different from the damped propagation predicted by common hyperbolic models. A fit of the density profiles is finally presented.

Index Terms—Transport phenomena, probabilistic modelling, simulation

I. INTRODUCTION

Transport at bounded velocity is encountered in many different contexts which range from metal [17], [13] and computer engineering [3] to tumor treatment [16], [14] and fusion plasma physics [18], [10]. Finding realistic models of such transport is a long standing problem of continuous media theories [2], [12], [19], [11], [4]. The simplest form of transport is matter transport and the simplest models of matter transport are stochastic processes. Stochastic processes which bound the velocity of the diffusing matter have been introduced in [4]. We show here by an analytical computation that, for a very large and natural class of initial conditions, these processes display propagative (ballistic) behaviour at short times. This propagation (ballistic) effect contrasts sharply with (i) standard diffusive behaviour, which only appears at asymptotic large times (ii) damped propagation predicted by the widely used hyperbolic transport models based on the telegraph equation. We illustrate these findings by numerical simulations of the ROUP [8], which is the first bounded velocity process introduced in the physical literature. We finally present a simple analytical *Ansatz*, which fits the density of the ROUP at all times to an accuracy of order 3% and which can be used in a more general context to model bounded velocity transport.

II. SHORT-TIME PROPAGATIVE BEHAVIOUR OF BOUNDED VELOCITY PROCESSES

Consider the following 1D stochastic process:

$$dx_t = v_t dt \quad (1)$$

$$dv_t = F(v_t) dt + \sigma(v_t) dB_t \quad (2)$$

where F is a friction or dissipative term and σ is a noise coefficient. Equation (1) is simply the definition of the velocity v as the time-derivative of the position x and (2) is a generalization of Langevin equation.

Fabrice Debbasch: fabrice.debbasch@gmail.com,
David Espaze: davidespaze@yahoo.fr,
Vincent Foulonneau: vfoulonneau@hotmail.fr.
LERMA, UMR 8112, Université Pierre-et-Marie-Curie, 4 place
Jussieu, 75005 Paris, France.

Since we are modeling bounded velocity transport, we suppose that the initial condition and the process itself restricts v to a finite interval, say $I = (-c, +c)$, where c is an arbitrary constant velocity which depends on the nature of the diffusing particles and of the medium in which transport occurs. A simple one-to-one map of this interval onto \mathbf{R} is of course:

$$\begin{aligned} p : I &\rightarrow \mathbf{R} \\ v &\rightarrow p(v) = \gamma(v)v \end{aligned} \quad (3)$$

with $\gamma(v) = (1 - \frac{v^2}{c^2})^{-1/2}$. Note that $v \rightarrow \pm c$ corresponds to $p \rightarrow \pm\infty$ and $\gamma \rightarrow +\infty$. The first equation of the process transcribes into

$$dx_t = \frac{p_t}{\Gamma(p_t)} dt \quad (4)$$

with $\Gamma(p) = (1 + p^2/c^2)^{1/2}$. The variable p will henceforth be called the momentum of the diffusing particle.

Consider a diffusing particle starting its motion from point $x_0 = 0$ with initial momentum p_0 . For sufficiently small times, the position varies with time according to:

$$x_t = \frac{p_0}{\Gamma(p_0)} t + O(t^2). \quad (5)$$

The probability law of x_t and, thus, the density n are then entirely determined by the probability law of p_0 i.e. the initial momentum distribution of the particle, which we denote by $F^*(p)dp$. To make the discussion simpler, suppose that F^* is isotropic, and write $F^*(p) = \exp(-\Phi(\Gamma(p)))$.

Equations (4) and (5) show that x_t/t has the same probability law as the initial velocity of the particle. This law can be obtained by changing variables in the initial momentum distribution $F^*(p)$. By direct differentiation,

$$dp = (\gamma(v))^3 dv \quad (6)$$

and this leads to

$$n(t, x) \approx \frac{1}{t} \left(\gamma \left(\frac{x}{t} \right) \right)^3 \exp \left(-\Phi \left(\gamma \left(\frac{x}{t} \right) \right) \right). \quad (7)$$

The maxima and minima of n at short time can be identified by computing the first and second derivatives of this expression with respect to x . One finds that, for all increasing function Φ such that the equation $\gamma\Phi'(\gamma) = 3$ admits a single solution γ^* , the points $\pm x^*(t) = \pm c^*t$ with $c^* = c\sqrt{1 - 1/\gamma^{*2}}$ are maxima of the density provided the function Φ is convex¹. Thus, for any convex function Φ , the short-time density profile exhibits two peaks which travel at constant velocity c^* . The short-time transport thus exhibits propagative (ballistic) behaviour.

¹this last condition is sufficient but not necessary for the extrema at $\pm x^*(t)$ to be maxima. The necessary and sufficient condition is $D^* = -3\gamma^* - \gamma^{*3}\Phi''(\gamma^*) < 0$

III. ILLUSTRATION THROUGH NUMERICAL SIMULATIONS

The ROUP [8], [6] corresponds to the choices $F(v) = -\alpha v$ and $\sigma(v) = \sqrt{2D}$, where α and D are both constant. The constant α is a friction coefficient, and D is a noise coefficient. Numerical simulations have been performed for the one-parameter family of functions Φ :

$$\Phi_\beta(\gamma) = \beta\gamma + a(\beta), \tag{8}$$

where β is an arbitrary real positive coefficient and $a(\beta)$ ensures that the corresponding initial momentum distribution F_β^* is normalized to unity with respect to dp . This distribution is a hyperbolic distribution commonly called Jüttner distribution [15], [5] and β plays the role of an initial inverse temperature for the ROUP. At fixed p and thus, at fixed value of $\Gamma(p)$, the ratio $A_\beta(p) = F_\beta^*(p)/F_\beta^*(0)$ decreases exponentially as β increases. For $\beta \gg 1$, $A_\beta(p)$ is comparable to unity only if $p \ll c$. This means that the diffusing particle, initially, does not ‘see’ the maximum velocity c ; note that, for $p \ll c$, the function $\Gamma(p)$ can be approximated by its expansion around $p = 0$ i.e. $\Gamma(p) \simeq 1 + p^2/(2c^2)$ and F_β^* is then approximately Gaussian.

Figures 1 and 2 display typical profiles for the density n_β generated by the ROUP with initial condition (8). Figure 1 displays $n_{\beta=1}$ as a function of $\xi = ct$ for different values of the dimensionless time $T = \alpha t$.

At early times, the maximum of the density profile is not situated at $\xi = 0$ i.e. at the starting point of the diffusion, but rather at $|\xi_{\beta=1}| \approx 0.948$, remarkably close to the analytical prediction $|x_\beta^*(t)/(ct)| = |\xi_\beta^*(t)| = 0.943$ (see Section II. above). In time, a secondary maximum appears at the origin point $\xi = 0$. This secondary maximum grows and finally becomes much higher than the peaks at $\pm\xi_{\beta=1}$. The density profile thus gets closer and closer to a Gaussian and the bounded velocity transport transforms into standard diffusion with diffusion coefficient $\chi = D/\alpha^2$ in physical space, as expected from [9], [1].

Fix now an arbitrary, not necessarily large dimensionless time T and consider the density profile $n_\beta(T, \cdot)$ at this time. As β tends to infinity, this density profile also tends towards the standard diffusion Gaussian. Indeed, the more β increases, the less the diffusing particle ‘sees’ the velocity bound c (see the discussion above) and the more the transport looks like standard Fickian diffusion. Note also that the time at which the secondary maximum appears at the origin is a decreasing function of β and tends to zero as β tends to infinity.

IV. FAILURE OF THE HYPERBOLIC DIFFUSION MODEL

Let us show that the spatial density of the ROUP does not obey Cattaneo’s hyperbolic diffusion equation [2], which is a popular model of bounded speed transport. Cattaneo’s damped wave equation reads:

$$\partial_t n = \chi \square n = \chi \left(\partial_{xx} - \frac{1}{c^2} \partial_{tt} \right) n, \tag{9}$$

where \square is the D’Alembert operator with velocity c and $\chi = D/\alpha^2$ is the usual diffusion coefficient in position space. We have computed numerically the relative discrepancy $R_\beta(T)$ between $\partial_t n_\beta$ and $\chi \square n_\beta$; Figure 3 displays a typical

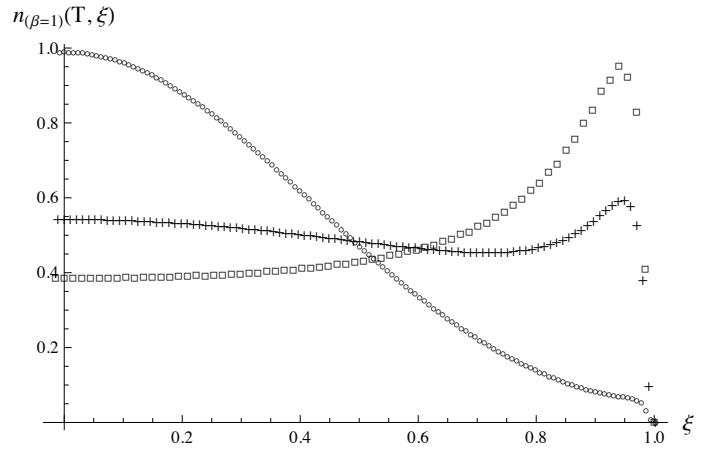


Fig. 1. **Density profile and propagation.** Density-profile n_β against rescaled position $\xi = x/(ct)$ for $\beta = 1$ and $T = \alpha t = 0.5$ (squares), $T = 2$ (crosses) and $T = 10$ (circles). The density n_β is normalized to unity with respect to $d\xi$.

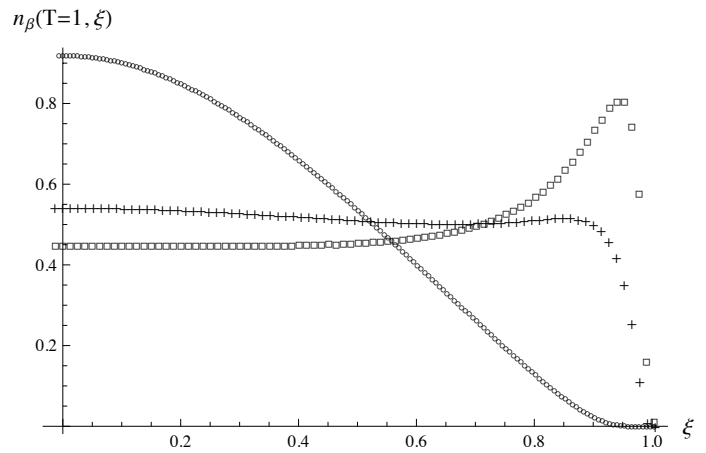


Fig. 2. **Density profile and propagation.** Density-profile n_β against rescaled position $\xi = x/(ct)$ for $T = 1$ and $\beta = 1$ (squares), $\beta = 1.2$ (crosses) and $\beta = 2$ (circles). The density n_β is normalized to unity with respect to $d\xi$.

result in Fourier space. This figure clearly displays the failure of Cattaneo’s hyperbolic diffusion model to reproduce the correct density profile of the ROUP.

V. FIT OF THE DENSITY PROFILE

Consider now the following function of position and time:

$$N_{\alpha,\sigma,B}(t, x) = B(t) \left(\gamma \left(\frac{x}{t} \right) \right)^{\alpha(t)} \exp \left(-\phi_Q \left(\gamma \left(\frac{x}{t} \right) \right) \right) \times \exp \left(-\frac{x^2}{2\sigma(t)^2} \right), \tag{10}$$

where α and σ are two arbitrary functions of t and B ensures that $N_{\alpha,\sigma,B}$ is at all times normalized to unity on $(-ct, ct)$.

At each time t , the values of $\alpha_\beta(t)$, $\sigma_\beta(t)$ and $B_\beta(t)$ producing the best fits of n_β can be obtained, for example, by minimizing the following distance function $d_C(t)$ between $n_\beta(t, \cdot)$ and $N_{\alpha\sigma B}(t, \cdot)$:

$$d_C(T) = \int_{\mathbf{R}} |n_\beta(t, x) - N_{\alpha\sigma B}(t, x)| dx + \lambda_B \left| 1 - \int_{\mathbf{R}} N_{\alpha\sigma B}(t, x) dx \right|, \tag{11}$$

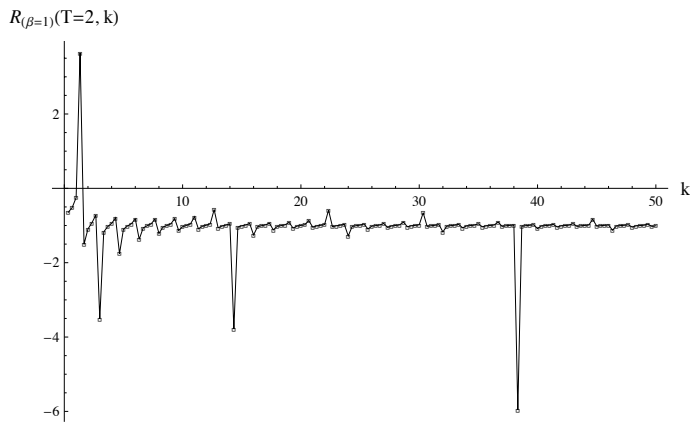


Fig. 3. **Failure of the hyperbolic diffusion model.** Evolution with k of the relative discrepancy between $\partial_t n_\beta$ and $\chi \square n_\beta$ for $\beta = 1$ and $T = 2$. The hyperbolic Cattaneo model predicts R identically vanishes.

where λ_B is a Lagrange multiplier which enforces normalization and the convention $N_{\alpha\sigma B}(t, x) = 0$ for $|x| > ct$ has been used.

Figures 4, 5 and 6 display the results of the fit at different times for $\beta = 1$ and $\lambda_B = 100$. The precision of the fit is always better than 3% (see Figure 6). The coefficient α_β remains close to the above computed value of 3 and seems to globally decrease with time; its average value for the points plotted in Figure 4 is 2.88. At small times, $\sigma_\beta(t)$ behaves like $2\sqrt{t}/3$ (see the green dashed curve in Figure 5) and is thus larger than ct (the red straight line in Figure 5); the Gaussian then varies slowly over $(-ct, +ct)$, the shape of the density profile is essentially controlled by the $\gamma^{\alpha_\beta(t)} \exp(-\beta\gamma)$ and it thus displays the characteristic peaks x close to ct . As t increases, $\sigma_\beta(t)$ becomes smaller than ct and the maximum of the Gaussian at $x = 0$ generates the secondary maximum at $x = 0$. As time still increases, $\sigma_\beta(t)$ increases slowly from $2\chi\sqrt{t}/3$ to $\chi\sqrt{t}$ (the onset of this increase can actually be seen in Figure 5) but $\sigma_\beta(t)/(ct)$ continues to decrease towards zero; the density profile is then essentially controlled by the Gaussian and tends towards the standard result predicted by Fick's law.

Let us stress that the fit presented in this section is not based on an approximate analytical computation of the finite-time density profile, but is only a heuristic extension of the short-time computation presented in the previous section. This fit nevertheless highlights the fact that the whole time-evolution of the density profile can be understood in very simple terms *i.e.* as the superposition of two competing phenomena which are (i) the propagation of the peaks at velocity close to the light-velocity (ii) a standard Gaussian diffusion with a typical scaling as \sqrt{t} .

The fit also constitutes a simple, ready-to-use model of finite speed transport. It can be easily integrated into numerical simulations and should thus prove useful in a wide variety of physical and engineering applications.

VI. DISCUSSION

We have proved that bounded velocity diffusions exhibit short-time propagative behaviour for a wide class of initial conditions. This has been illustrated by numerical simulations of the ROUP. We have also shown numerically that the widely used hyperbolic diffusion model does not replicate the

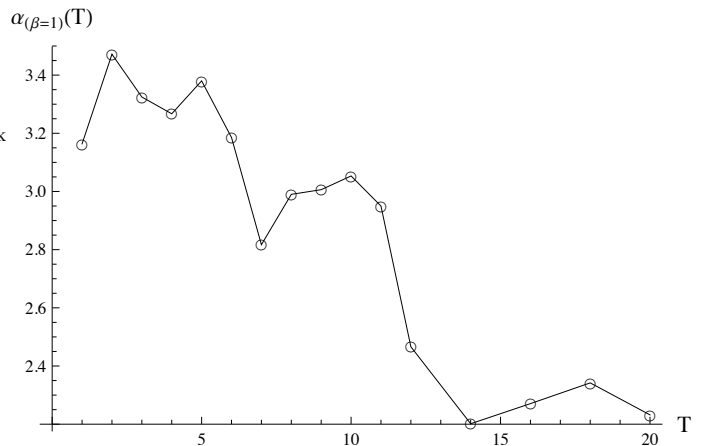


Fig. 4. **Fit of the density profile.** Time-evolution of the α -coefficient for $\beta = 1$.

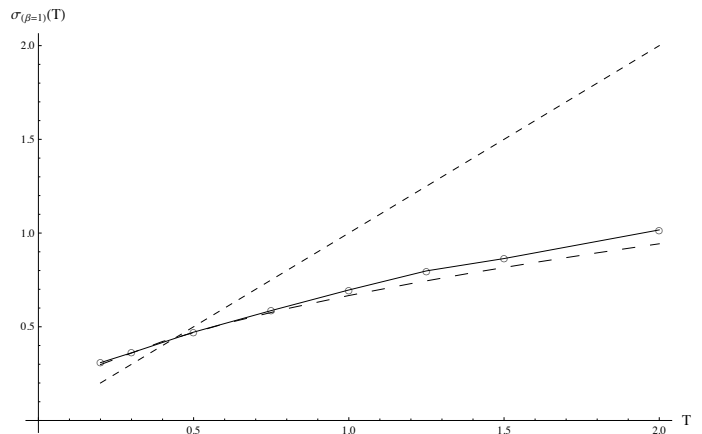


Fig. 5. **Fit of the density profile.** Time-evolution of the σ -coefficient (circles) for $\beta = 1$. The straight line is $x = ct$ and the dashed curve is $x = (2/3)\chi\sqrt{t}$.

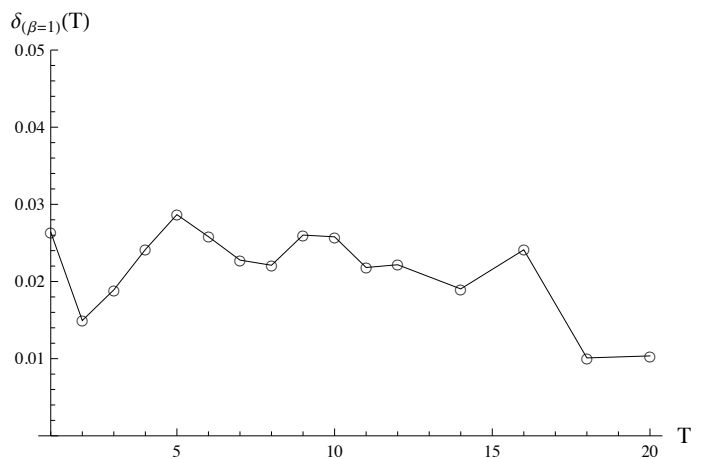


Fig. 6. **Fit of the density profile.** Time-evolution of the absolute error of the fit for $\beta = 1$.

density profiles of the ROUP and we have finally presented a simple *Ansatz* which fits these profiles to a precision better than 3%.

We believe several general conclusions can be drawn from these results. First, the failure of the hyperbolic diffusion model to replicate the density profile of the ROUP, which is certainly the simplest reliable model of bounded velocity transport, strongly suggests that this model also fails in more complicated problems involving mass transport as well as momentum viscous transport and heat conduction.

The material presented in this article indicates (i) that bounded velocity effects are essentially short-time effects (ii) that these effects depend on all characteristics of the initial state of the system in which transport is to occur. Indeed, in the situation studied in this article, the short-time density profile depends, not only on the initial position of the diffusing particle, but also on its initial velocity distribution and, in particular, on its initial temperature.

Let us mention here that the density profiles of bounded velocities processes can be derived from a geometrical generalization of the standard Fick's law. Reference [7] presents this generalization for the ROUP.

Finally, all the results presented in this article need to be extended properly to include viscous momentum transfer and heat conduction. This can be accomplished, at least in theory, by analyzing kinetic models richer than the ROUP which also bound particle velocities.

Acknowledgements: Part of this work was funded by the ANR Grant 09-BLAN-0364-01.

REFERENCES

- [1] J. Angst and J. Franchi. Central limit theorem for a class of relativistic diffusions. *J. Math. Phys.*, 48(8), 2007.
- [2] C. Cattaneo. Sulla conduzione del calore. *Atti Sem. Mat. Fis. Univ. Modena*, 3, 1948.
- [3] H.T. Chen, J.P. Song, and K.C. Liu. Study of Hyperbolic heat Conduction Problem in IC Chip. *Japanese Journal of Applied Physics*, 43 (7A):4404-4410, 2004.
- [4] C. Chevalier, F. Debbasch, and J.P. Rivet. A review of finite speed transport models. In *Proceedings of the Second International Forum on Heat Transfer (IFHT08), Sept. 17-19, Tokyo, Japan*. Heat Transfer Society of Japan, 2008.
- [5] F. Debbasch. Equilibrium distribution function of a relativistic dilute perfect gas. process. *Physica A*, 387:2443-2454, 2008.
- [6] F. Debbasch and C. Chevalier. Relativistic stochastic processes. *Proceedings of XV Conference on Non-equilibrium Statistical Mechanics and Nonlinear Physics, Mar del Plata, Argentina, Dec. 4-8 2006 A.I.P. Conference Proceedings*, 2007.
- [7] F. Debbasch, G. Di Molfetta, D. Espaze and V. Foulonneau. Propagation in quantum walks and relativistic diffusions. *Accepted for publication in Physica Scripta*, 2012.
- [8] F. Debbasch, K. Mallick, and J.P. Rivet. Relativistic Ornstein-Uhlenbeck process. *J. Stat. Phys.*, 88:945, 1997.
- [9] F. Debbasch and J.P. Rivet. A diffusion equation from the relativistic Ornstein-Uhlenbeck process. *J. Stat. Phys.*, 90:1179, 1998.
- [10] J. Freidberg. *Plasma Physics and Fusion Energy*. Cambridge, 2007.
- [11] L. Herrera and D. Pavon. Why hyperbolic theories of dissipation cannot be ignored: Comments on a paper by Kostadt and Liu. *Phys. rev. D*, 64:088503, 2001.
- [12] W. Israel. Covariant fluid mechanics and thermodynamics: An introduction. In A. Anile and Y. Choquet-Bruhat, editors, *Relativistic Fluid Dynamics*, volume 1385 of *Lecture Notes in Mathematics*, Berlin, 1987. Springer-Verlag.
- [13] T.E. Itina, M. Mamatkulov, and M. Sentis. Nonlinear fluence dependencies in femtosecond laser ablation of metals and dielectrics materials. *Optical Engineering*, 44 (5):051109-051116, 2005.
- [14] M.K. Jaunich et al. Bio-heat transfer analysis during short pulse laser irradiation of tissues. *Intl.J.Heat and Mass Transfer*, 51:5511-5521, 2006.
- [15] F. Jüttner. Das Maxwellsche Gesetz der Geschwindigkeitsverteilung in der Relativtheorie. *Ann. Phys. (Leipzig)*, 34:856, 1911.
- [16] K. Kim and Z. Guo. Multi-time-scale heat transfer modeling of turbid tissues exposed to short-pulse irradiations. *Computer Methods and Programs in Biomedicine*, 86 (2):112-123, 2007.
- [17] J.J. Klossika, U. Gratzke, M. Vicanek, and G. Simon. Importance of a finite speed of heat propagation in metal irradiated by femtosecond laser pulses. *Phys. Rev. B*, 54 (15):10277-10279, 1996.
- [18] J.R. Martin-Solis et al. Enhanced production of runaway electrons during a disruptive termination of discharges heated with lower hybrid power in the Frascati tokamak upgrade. *Phys. Rev. Lett.*, 97:165002, 2006.
- [19] I. Müller and T. Ruggeri. *Extended Thermodynamics*, volume 37 of *Springer Tracts in Natural Philosophy*. Springer-Verlag, New-York, 1993.